An initial-boundary value problem for the Korteweg-de Vries equation on the negative quarter-plane.

J.A. Leach[1] and S. Shaw[2]

[1]School of Mathematics, University of Birmingham, Edgbaston, Birmingham, B15 2TT, UK

[2]Mathematical Sciences, Brunel University, Uxbridge, Middlesex, UB8 3PH, UK

August 22, 2009

Abstract

In this paper, we consider an initial-boundary value problem for the Korteweg-de Vries equation on the negative quarter-plane. The normalized Korteweg-de Vries equation considered is given by

$$u_\tau + uu_x + u_{xxx} = 0, \quad x < 0, \quad \tau > 0,$$

where x and τ represent dimensionless distance and time respectively. In particular, we consider the case when the initial and boundary conditions are given by $u(x,0) = u_i$ for $x < 0$ and $u(0,\tau) = u_b$, $\frac{\partial}{\partial x}u(0,\tau) = u_{bx}$ for $\tau > 0$. Here the initial value $u_i < 0$ and we restrict attention to boundary values u_b and u_{bx} in the ranges $0 < u_b < -2u_i$ and $|u_{bx}| \geq \frac{1}{\sqrt{3}}(u_b - u_i)(-u_b - 2u_i)^{\frac{1}{2}}$ respectively. The method of matched asymptotic coordinate expansions is used to obtain the large-τ asymptotic structure of the solution to this problem, which exhibits the formation of a dispersive shock wave when $|u_{bx}| > \frac{1}{\sqrt{3}}(u_b - u_i)(-u_b - 2u_i)^{\frac{1}{2}}$. We also present detailed numerical simulations of the full initial-boundary value problem which support the asymptotic analysis presented. A brief discussion is also given of the large-τ asymptotic structure to this problem when $u_i < 0$, $u_b \geq -2u_i$ and $u_{bx} \in (-\infty, \infty)$.

1 Introduction

In this paper we consider the following initial-boundary value problem for the normalized Korteweg-de Vries equation, namely,

$$u_\tau + uu_x + u_{xxx} = 0, \quad x < 0, \quad \tau > 0, \tag{1.1}$$

$$u(x,0) = u_i, \qquad x < 0, \tag{1.2}$$

$$u(0,\tau) = u_b, \qquad \tau > 0, \tag{1.3}$$

$$\frac{\partial}{\partial x}u(0,\tau) = u_{bx}, \quad \tau > 0, \tag{1.4}$$

where the initial value $u_i < 0$ and we restrict attention to boundary values u_b and u_{bx} in the ranges $0 < u_b < -2u_i$ and $|u_{bx}| \geq \frac{1}{\sqrt{3}}(u_b - u_i)(-u_b - 2u_i)^{\frac{1}{2}}$ respectively. In what follows we label initial-boundary value problem (1.1)-(1.4) as **IBVP**.

We note that the Korteweg-de Vries equation is a canonical equation combining both nonlinearity and dispersion and as such arises in the modelling of many physical phenomena including for example shallow-water gravity waves, ion-acoustic waves and

waves in the atmosphere and ocean. Clearly, the literature relating to the Korteweg-de Vries equation is vast and we make no attempt here to summarize it, rather we make reference only to the most salient to this present paper. The analysis of initial-boundary value problems on the positive quarter-plane has received considerable attention over recent years, and a review of some of the more significant literature in the area can be found in [11], [13] and [14]. In particular, in the recent paper [7] the large-time development of the solution to an initial-boundary value problem for the positive quarter-plane was considered in detail, using the method of matched coordinate expansions. However, the analysis of initial-boundary value problems on the negative quarter-plane is far less developed, although some excellent numerical studies exist (see for example [13] and [14]). Further, the well-posedness of negative quarter-plane problems has been addressed in, for example, [3] and [13] (and references therein). There are a number of physical applications, including weakly nonlinear long waves propagating on a fluid with surface tension [6], and the plasma-sheath transition layer [12].

In [8] (hereafter, referred to as L) the method of matched asymptotic coordinate expansions was used to develop the complete large-τ asymptotic structure of the solution to **IBVP** when $u_i < 0$ for boundary values u_b and u_{bx} in the ranges

(I) $0 < u_b < -2u_i, \ |u_{bx}| < \frac{1}{\sqrt{3}}(u_b - u_i)(-u_b - 2u_i)^{\frac{1}{2}}.$

The large-τ asymptotic structure of solution to **IBVP** in this case was obtained by careful consideration of the asymptotic structures as $\tau \to 0$ ($-\infty < x \leq 0$) and as $x \to -\infty$ ($\tau \geq O(1)$). The methodology used was analogous to that developed in the context of reaction-diffusion equations and is elucidated in [10]. The leading order structure of the solution to **IBVP** for $x = O(1)$ (≤ 0) was found to be the steady state solution

$$u_s(x) = u_l - 3u_l \, \text{sech}^2\left(\frac{\sqrt{-u_l}}{2}x \pm \text{sech}^{-1}\left(\frac{u_b - u_l}{-3u_l}\right)^{\frac{1}{2}}\right), \qquad (1.5)$$

with $x = O(1)$ (≤ 0), and where

$$u_l = \left(r_+ + r_- + \frac{1}{2}\right)u_b, \quad u_l \in \left(u_i, -\frac{u_b}{2}\right], \qquad (1.6)$$

with

$$r_\pm = \frac{1}{2u_b}\left(-6u_{bx}^2 - u_b^3 \pm 2\sqrt{3}\, u_{bx}\, \sqrt{3u_{bx}^2 + u_b^3}\right)^{\frac{1}{3}}. \qquad (1.7)$$

The $-$[+] sign in (1.5) is taken when u_{bx} is positive [negative] respectively. Further, the rate of convergence of the solution of **IBVP** to the steady state $u_s(x)$ was found to be exponential in τ as $\tau \to \infty$, with

$$u(x, \tau) = u_s(x) + O\left(\tau^{-\frac{3}{2}}\exp\left[-\frac{2}{3\sqrt{3}}(-u_l)^{\frac{1}{2}}\tau\right]\right) \qquad (1.8)$$

as $\tau \to \infty$ with $x = O(1)$ (≤ 0). This steady state solution is connected to the oscillatory behaviour (oscillating about u_i) when $x < u_i\tau$ by the expansion wave

$$u(x, \tau) \sim \frac{x}{\tau}, \quad x \in (u_i\tau, u_l\tau) \qquad (1.9)$$

as $\tau \to \infty$. We note that this expansion wave is connected to the steady state and oscillatory behaviour by localized connection regions, located at $x = u_l\tau$ and $x = u_i\tau$ respectively. The full details of these results are reported in L, which both confirm the numerical simulations presented in [13] and [14], and extend the analysis presented in [14].

2

The aim of this present paper is to extend the analysis presented in L by determining the complete large-τ structure of the solution to **IBVP** when $u_i < 0$ for boundary values u_b and u_{bx} in the ranges

(II) $0 < u_b < -2u_i,\ |u_{bx}| = \frac{1}{\sqrt{3}}(u_b - u_i)(-u_b - 2u_i)^{\frac{1}{2}}$

and

(III) $0 < u_b < -2u_i,\ |u_{bx}| > \frac{1}{\sqrt{3}}(u_b - u_i)(-u_b - 2u_i)^{\frac{1}{2}}.$

In each case the asymptotic analysis presented is supported by detailed numerical simulations. We conclude by giving a brief discussion of the large-τ asymptotic structure of the solution to **IBVP** when $u_i < 0$ and with boundary values u_b and u_{bx} in the ranges $u_b \geq -2u_i$ and $u_{bx} \in (-\infty, \infty)$. When $(u_b > -2u_i, u_{bx} \in (-\infty, \infty))$ or $(u_b = -2u_i, u_{bx} \neq 0)$ then $u_l < u_i$ and the large-τ asymptotic structure of the solution to **IBVP** follows, after minor modification, that given for case (III). However, when $(u_b = -2u_i, u_{bx} = 0)$ then $u_l = u_i$ and the large-τ asymptotic structure of the solution to **IBVP** follows, after minor modification, that given for case (II).

The large-τ solution to **IBVP** in case (III) contains a dispersive shock wave (undular bore). This dispersive shock wave is connected to the steady state (1.5) (where $u_l < u_i$ and is given by (1.6) and (1.7)) and the oscillatory behaviour when $x < (2u_l - u_i)\tau$ $\left(\text{where } u = u_i + O\left(\tau^{-\frac{1}{2}}\right) \text{ as } \tau \to \infty\right)$ by localized connection regions, located at $x = \left(\frac{2u_i}{3} + \frac{u_l}{3}\right)\tau$ and $x = (2u_l - u_i)\tau$ respectively. The rate of convergence of the solution to **IBVP** to the steady state $u_s(x)$ in this case is exponential in τ as $\tau \to \infty$, with

$$u(x, \tau) = u_s(x) + O\left(\exp\left[-\left(\frac{2}{3}\right)^{\frac{3}{2}}(u_i - u_l)^{\frac{1}{2}}\left(-u_i - \frac{u_l}{2}\right)\tau\right]\right) \qquad (1.10)$$

as $\tau \to \infty$ with $x = O(1)\ (\leq 0)$. The dispersive shock wave has been examined using Whitham's quasi-classical method (see [4], [5] and [15]) and the approximate solution of (1.1) when $x \in \left[(2u_l - u_i)\tau, \left(\frac{2}{3}u_i + \frac{u_l}{3}\right)\tau\right]$ for $\tau \gg 1$ (within which the Whitham equations are valid) connecting $u = u_i$ to $u = u_l$, is given (up to an arbitrary phase shift) by

$$u(x, \tau) = 2(u_i - u_l)\ \text{dn}^2\left[\sqrt{\frac{u_i - u_l}{6}}\left(x - \frac{1}{3}\left[(1 + m^2)(u_i - u_l) + 3u_l\right]\tau\right), m\right]$$
$$- (1 - m^2)(u_i - u_l) + u_l, \qquad (1.11)$$

where $\text{dn}[., m]$ is the standard Jacobian elliptic function (see [1], pp. 569-581) with modulus m $(0 \leq m \leq 1)$. The modulus is a function of x/τ and is determined by the modulation equation

$$\frac{1}{3}(1 + m^2)(u_i - u_l) + u_l - \frac{2}{3}\frac{(u_i - u_l)m^2(1 - m^2)\text{K}(m)}{\text{E}(m) - (1 - m^2)\text{K}(m)} = \frac{x}{\tau} = y, \qquad (1.12)$$

where $\text{K}(m)$, $\text{E}(m)$ are the standard complete elliptic integrals of the first and second kind respectively. The group velocity, v_g, at the front (when $m = 1$) and rear (when $m = 0$) of the dispersive shock wave are given by $\frac{2u_i}{3} + \frac{u_l}{3}$ and $(2u_l - u_i)$ respectively. We note that the wave number, k, is given by

$$k = \frac{\pi}{K(m)}\sqrt{\frac{u_i - u_l}{6}}, \qquad (1.13)$$

3

while the mean height, $u_{\bar{h}}$, phase velocity, v_p, and wave envelope, u_e, of this oscillatory solution are given by

$$u_{\bar{h}} = -(1 - m^2)(u_i - u_l) + u_l + 2(u_i - u_l)\frac{E(m)}{K(m)}, \qquad (1.14)$$

$$v_p = \frac{1}{3}(1 + m^2)(u_i - u_l) + u_l, \qquad (1.15)$$

and

$$u_e = u_i \pm m^2(u_i - u_l). \qquad (1.16)$$

Finally, It follows from (1.12) that as $m \to 1^-$ $\left(\text{that is, as } y \to \left(\frac{2u_i}{3} + \frac{u_l}{3}\right)^-\right)$ we approach the the front of the wave (the soliton limit) and the oscillations break up and approach solitons. In particular, via (1.11), we have that

$$u(y, \tau) = u_l + 2(u_i - u_l) \operatorname{sech}^2\left(\sqrt{\frac{u_i - u_l}{6}}\left(y - \left[\frac{2u_i}{3} + \frac{u_l}{3}\right]\right)\tau\right) + O\left(1 - m^2\right) \qquad (1.17)$$

as $m \to 1^-$. We note from (1.17) that the leading soliton has amplitude $2(u_i - u_l)$ and speed $\frac{2u_i}{3} + \frac{u_l}{3}$. Further, as $m \to 0^+$ $\left(\text{that is, as } y \to (2u_l - u_i)^+\right)$ we approach the rear of the wave (the harmonic limit) and the solution approaches linear oscillations about u_i, with phase velocity

$$v_p = \frac{1}{3}(u_i + 2u_l) \qquad (1.18)$$

and wave number

$$k = \sqrt{\frac{2(u_i - u_l)}{3}}. \qquad (1.19)$$

The full details of the large-τ asymptotic structure of the solution to **IBVP** in this case are reported in Section 2.3.2.

The final case, case (II), separates the distinct large-τ structures of the solution to **IBVP** in cases (I) and (III). In this case the oscillatory behaviour when $x < u_i\tau$ is connected to the steady state solution (1.5) (with $u_l = u_i$) via a localized connection region, located at $x = u_i\tau$. The rate of convergence of the solution to **IBVP** to the steady state $u_s(x)$ is given by (1.8) (with $u_l = u_i$). The full details of this case are reported in Section 2.3.1.

We conclude by noting that the methodology presented in this paper for initial-boundary value problem **IBVP** is applicable to a large class of nonlinear evolution equations. In particular, where a coherent structure forms the large-time attractor for the solution to initial-value (or initial-boundary value) problem for a nonlinear evolution equation (or system of equations).

2 Asymptotic solution to IBVP as $\tau \to \infty$

To develop the asymptotic structure of the solution to **IBVP** as $\tau \to \infty$, we must follow L and first consider both the asymptotic structures to the solution of **IBVP** as $\tau \to 0$ followed by $x \to -\infty$. The details are as in L, and we repeat here only the overall results.

2.1 Asymptotic solution to IBVP as $\tau \to 0$

Following L, the asymptotic structure of the solution to **IBVP** as $\tau \to 0$ has two regions. We have:

4

Region **I** $x = o(1)$ as $\tau \to 0$

$\eta = x\tau^{-\frac{1}{3}} = O(1)$ (≤ 0) as $\tau \to 0$ and,

$$u(\eta, \tau) = u_b - \frac{3}{2}(u_b - u_i)\int_{\eta 3^{-\frac{1}{3}}}^{0} \text{Ai}(s)\mathrm{d}s$$

$$- \sqrt{3}\left[\Gamma\left(\frac{2}{3}\right)u_{bx} - \frac{(u_b - u_i)}{2}\right]\int_{\eta 3^{-\frac{1}{3}}}^{0} \text{Bi}(s)\mathrm{d}s + o(1) \qquad (2.1)$$

as $\tau \to 0$ with $\eta = O(1)$ (≤ 0), where Ai[.] and Bi[.] are the standard Airy functions (see [1], pp. 446-450).

Region **II** $x = O(1)$ (< 0) as $\tau \to 0$

$$u(x, \tau) = u_i + \exp\left(i\frac{2}{3\sqrt{3}}(-x)^{\frac{3}{2}}\tau^{-\frac{1}{2}} + \frac{1}{4}\ln\tau + \left[i\left(\frac{\pi}{4} + \tan^{-1}\left(\frac{A_s}{A_c}\right)\right) - \frac{3}{4}\ln(-x)\right.\right.$$

$$\left.\left. + \frac{1}{2}\ln\left(\frac{A_c^2 + A_s^2}{4}\right)\right] + \tau^{\frac{1}{2}}\left[i\frac{u_i}{\sqrt{3}}(-x)^{\frac{1}{2}} + \ldots\right] + o\left(\tau^{\frac{1}{2}}\right)\right)$$

$$+ \exp\left(-i\frac{2}{3\sqrt{3}}(-x)^{\frac{3}{2}}\tau^{-\frac{1}{2}} + \frac{1}{4}\ln\tau + \left[-i\left(\frac{\pi}{4} + \tan^{-1}\left(\frac{A_s}{A_c}\right)\right)\right.\right.$$

$$\left.\left. - \frac{3}{4}\ln(-x) + \frac{1}{2}\ln\left(\frac{A_c^2 + A_s^2}{4}\right)\right] + \tau^{\frac{1}{2}}\left[-i\frac{u_i}{\sqrt{3}}(-x)^{\frac{1}{2}} + \ldots\right] + o\left(\tau^{\frac{1}{2}}\right)\right)$$

$$(2.2)$$

as $\tau \to 0$ with $x = O(1)$ (< 0), where

$$A_c = \frac{3^{\frac{5}{4}}(u_b - u_i)}{2\sqrt{\pi}} \qquad (2.3)$$

and

$$A_s = \frac{3^{\frac{3}{4}}}{\sqrt{\pi}}\left[\Gamma\left(\frac{2}{3}\right)u_{bx} - \frac{(u_b - u_i)}{2}\right]. \qquad (2.4)$$

The asymptotic structure as $\tau \to 0$ is now complete, with the expansions in regions **I** and **II** providing a uniform approximation to the solution of **IBVP** as $\tau \to 0$.

2.2   Asymptotic solution to IBVP as $x \to -\infty$

Following L, we have,

Region **III** $\tau = O(1)$ as $x \to -\infty$

$$u(x, \tau) = u_i + \exp\left(i\frac{2}{3\sqrt{3}}(-x)^{\frac{3}{2}}\tau^{-\frac{1}{2}} + i\frac{u_i}{\sqrt{3}}(-x)^{\frac{1}{2}}\tau^{\frac{1}{2}} - \frac{3}{4}\ln(-x)\right.$$

$$\left. + \left[i\left(\frac{\pi}{4} + \tan^{-1}\left(\frac{A_s}{A_c}\right)\right) + \frac{1}{4}\ln\tau + \frac{1}{2}\ln\left(\frac{A_c^2 + A_s^2}{4}\right)\right] + o\left(1\right)\right)$$

$$+ \exp\left(-i\frac{2}{3\sqrt{3}}(-x)^{\frac{3}{2}}\tau^{-\frac{1}{2}} - i\frac{u_i}{\sqrt{3}}(-x)^{\frac{1}{2}}\tau^{\frac{1}{2}} - \frac{3}{4}\ln(-x)\right.$$

$$\left. + \left[-i\left(\frac{\pi}{4} + \tan^{-1}\left(\frac{A_s}{A_c}\right)\right) + \frac{1}{4}\ln\tau + \frac{1}{2}\ln\left(\frac{A_c^2 + A_s^2}{4}\right)\right] + o\left(1\right)\right)$$

$$(2.5)$$

5

as $x \to -\infty$ with $\tau = O(1)$. Expansion (2.5) remains uniform for $\tau \gg 1$ provided that $(-x) \gg \tau$, but becomes nonuniform when $(-x) = O(\tau)$ as $\tau \to \infty$.

2.3 Asymptotic solution to IBVP as $\tau \to \infty$

As $\tau \to \infty$, the asymptotic expansion in region **III** continues to remain uniform for $(-x) \gg \tau$. However, as already noted, a nonuniformity develops when $(-x) = O(\tau)$. As in L, we proceed by introducing region **IV** in which $y = x/\tau = O(1)$ as $\tau \to \infty$.

To examine region **IV** we introduce the scaled coordinate $y = \frac{x}{\tau}$, where $y = O(1)$ ($<$ 0) as $\tau \to \infty$, and write (as suggested by (2.5))

$$u(x,\tau) = u_i + \left(e^{g^+(y,\tau)} + e^{g^-(y,\tau)} \right) \quad \text{as} \quad \tau \to \infty, \tag{2.6}$$

where

$$g^{\pm}(y,\tau) = \pm i g_0(y)\tau + g_1(y)\ln \tau \pm i g_2(y) + g_3(\tau) + o\,(1)\,, \tag{2.7}$$

as $\tau \to \infty$, with $y = O(1)$ (< 0). It is instructive to first consider the leading order problem in region **IV**. On substituting (2.6) and (2.7) into equation (1.1) (when written in terms of y and τ) we obtain the leading order problem as

$$\left(g_0'\right)^3 + (y - u_i)\,g_0' - g_0 = 0, \quad y < 0, \tag{2.8}$$

$$g_0(y) = \frac{2}{3\sqrt{3}}(-y)^{\frac{3}{2}} + \frac{u_i}{\sqrt{3}}(-y)^{\frac{1}{2}} + o\left[(-y)^{\frac{1}{2}}\right] \quad y \to -\infty. \tag{2.9}$$

The final condition, (2.9), arises from matching (2.6) ($(-y) \gg 1$) with expansion (2.5) ($-x = O(\tau)$). Equation (2.8) has a one-parameter family of linear solutions,

$$g_0(y) = -\alpha \left(y + \alpha^2 - u_i\right), \quad y \in (-\infty, \infty), \tag{2.10}$$

for each $\alpha \in \mathbb{R}$, together with the associated pair of envelope solutions,

$$g_0(y) = \pm \frac{2}{3\sqrt{3}}\left(u_i - y\right)^{\frac{3}{2}}, \quad y \in (-\infty, u_i]. \tag{2.11}$$

Combinations of (2.10) and (2.11) which remain continuous and differentiable also provide solutions to (2.8) (envelope touching solutions). The problem (2.8),(2.9) thus has a one-parameter family of solutions, namely, the envelope solution

$$g_0(y) = \frac{2}{3\sqrt{3}}\left(u_i - y\right)^{\frac{3}{2}}, \quad y \le u_i, \tag{2.12}$$

together with the family of envelope touching solutions, given by,

$$g_0(y, \alpha) = \begin{cases} \frac{2}{3\sqrt{3}}\left(u_i - y\right)^{\frac{3}{2}}, & y \le y_T(\alpha, u_i) \\ -\alpha \left(y - \left[u_i - \alpha^2\right]\right), & y_T(\alpha, u_i) < y < u_i - \alpha^2 \end{cases} \tag{2.13}$$

for each $\alpha > 0$, where,

$$y_T(\alpha, u_i) = u_i - 3\alpha^2. \tag{2.14}$$

Each of the above solutions is illustrated in Figure 1. Since the solution to (2.8) and (2.9) approaches zero as

$$y \to y_c(\alpha, u_i) = \begin{cases} u_i, & \alpha = 0 \\ u_i - \alpha^2, & \alpha > 0 \end{cases}, \tag{2.15}$$

then the expansion (2.6) with (2.7) becomes nonuniform as $y \to y_c^-(\alpha, u_i)$, specifically when

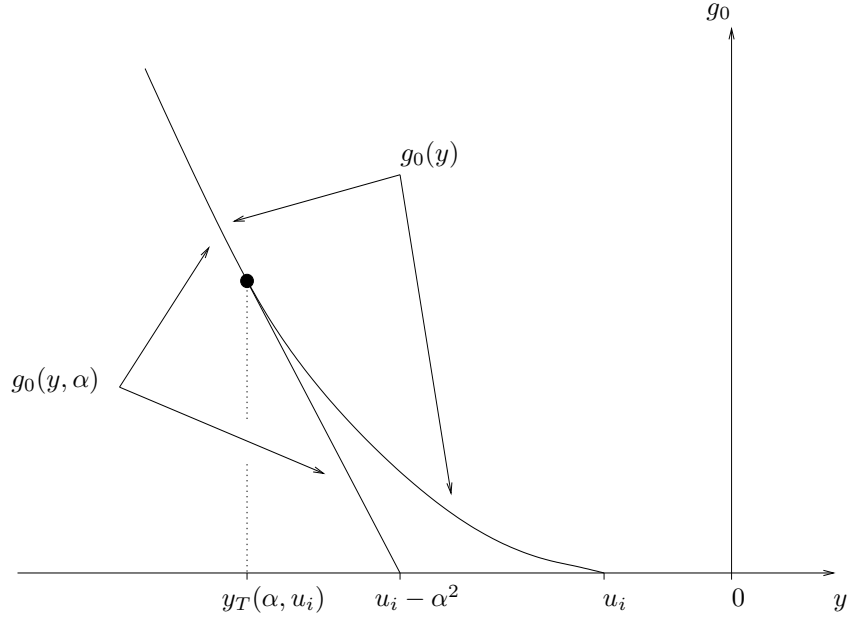$$y = y_c(\alpha, u_i) + O\big(\delta(\tau, \alpha)\big), \tag{2.16}$$

6

Figure 1: A sketch of $g_0(y)$ illustrating the envelope touching solution $g_0(y, \alpha)$ (given by (2.13)) and the full envelope solution $g_0(y)$ (given by (2.12)). We note that $y_T(\alpha, u_i) = u_i - 3\alpha^2$.

with

$$\delta(\tau, \alpha) = \begin{cases} \tau^{-1}, & \alpha > 0, \\ \tau^{-\frac{2}{3}}, & \alpha = 0. \end{cases} \tag{2.17}$$

We again note that when $\alpha > 0$, although $g_0(y, \alpha)$ and $g_0'(y, \alpha)$ are continuous over the range of definition $y \le y_c(\alpha, u_i)$, the second derivative $g_0''(y, \alpha)$ is discontinuous at the point at which the linear solution meets the envelope solution, that is at $y = y_T^-(\alpha, u_i)$. This indicates that a thin transition region exists in a neighbourhood of $y = y_T^-(\alpha, u_i)$ in which third order derivatives are retained at leading order to smooth out the discontinuity in curvature.

In L, when considering the parameter range (I) it was determined that $\alpha = 0$ with the large-τ structure of the solution to **IBVP** containing an expansion wave. However, in this present paper our aim is to extend the analysis presented in L by developing the large-τ structure of the solution to **IBVP** in cases (II) and (III). As already noted the large-τ structure of the solution of **IBVP** in these cases is distinct and in what follows they must be considered separately. We begin with case (II).

2.3.1 Case (II) $0 < u_b < -2u_i$, $|u_{bx}| = \frac{1}{\sqrt{3}}(u_b - u_i)(-u_b - 2u_i)^{\frac{1}{2}}$

In this case, $\alpha = 0$, and continuing expansion (2.6) results in,

$$g_1(y) = -\frac{1}{2}, \quad y < 0, \tag{2.18}$$

with $g_2(y)$ and $g_3(y)$ remaining indeterminate $O(1)$ functions, where

$$g_3(y) \sim -\frac{3}{4}\ln(-y) + \frac{1}{2}\ln\left(\frac{A_s^2 + A_c^2}{4}\right), \quad g_2(y) \sim \frac{\pi}{4} + \tan^{-1}\left(\frac{A_s}{A_c}\right) \quad \text{as} \quad y \to -\infty.$$

Thus we have, in region **IV**,

$$u(y, \tau) = u_i + \frac{\bar{g}_3(y)}{\tau^{\frac{1}{2}}}\cos\left(\frac{2}{3\sqrt{3}}(u_i - y)^{\frac{3}{2}}\tau + g_2(y)\right) + o\left(\frac{1}{\tau^{\frac{1}{2}}}\right) \tag{2.19}$$

7

as $\tau \to \infty$ with $y = O(1)$ $(\in (-\infty, u_i))$ and $\bar{g}_3(y) = \exp(g_3(y))$. Expansion (2.19) becomes nonuniform as $y \to u_i^-$. We must now introduce localized region **C** in which $y = u_i + O\left(\tau^{-\frac{2}{3}}\right)$ as $\tau \to \infty$. Thus we write

$$y = u_i + \frac{\zeta}{\tau^{\frac{2}{3}}} \tag{2.20}$$

in region **C**, with $\zeta = O(1)$ as $\tau \to \infty$. It follows from (2.20) and expansion (2.19) in region **IV**, that we should expand as

$$u(\zeta, \tau) = u_i + \psi(\tau)\bar{G}(\zeta) + o\left(\psi(\tau)\right) \quad \text{as} \quad \tau \to \infty \tag{2.21}$$

with $\zeta = O(1)$, and the gauge function

$$\psi(\tau) = o(1) \quad \text{as} \quad \tau \to \infty \tag{2.22}$$

is to be determined. On rewriting equation (1.1) in terms of ζ and substituting from (2.21) we obtain

$$\psi'(\tau)\bar{G} - \frac{1}{3}\frac{\psi(\tau)}{\tau}\zeta\bar{G}_\zeta + \frac{\psi^2(\tau)}{\tau^{\frac{1}{3}}}\bar{G}\bar{G}_\xi + \frac{\psi(\tau)}{\tau}\bar{G}_{\xi\xi} = 0. \tag{2.23}$$

A nontrivial balance requires

$$\frac{\psi^2(\tau)}{\tau^{\frac{1}{3}}} \sim \frac{\psi(\tau)}{\tau} \quad \text{as} \quad \tau \to \infty, \tag{2.24}$$

and so, without loss of generality, we take,

$$\psi(\tau) = \tau^{-\frac{2}{3}}. \tag{2.25}$$

We observe that all terms in (2.23) are retained at leading order as $\tau \to \infty$ and (2.23) becomes

$$\bar{G}_{\zeta\zeta\zeta} + \bar{G}\bar{G}_\zeta - \frac{\zeta}{3}\bar{G}_\zeta - \frac{2}{3}\bar{G} = 0, \quad -\infty < \zeta < \infty. \tag{2.26}$$

We note that equation (2.26) admits the solution $\bar{G}(\zeta) = \zeta$. The matching condition between expansion (2.21) with (2.25), and expansion (2.19) in region **IV** then requires

$$\bar{G}(\zeta) \sim \tilde{u}_\infty \, (-\zeta)^{\frac{1}{4}} \, \cos\left(\frac{2}{3\sqrt{3}}(-\zeta)^{\frac{3}{2}} + \tilde{\theta}_\infty\right) \quad \text{as} \quad \zeta \to -\infty. \tag{2.27}$$

We observe that

$$\bar{g}_3(y) \sim \tilde{u}_\infty \, (u_i - y)^{\frac{1}{4}}, \quad g_2(y) \sim \tilde{\theta}_\infty \quad \text{as} \quad y \to u_i^-,$$

where the constants $\tilde{u}_\infty > 0$ and $\tilde{\theta}_\infty$ are undetermined at this stage. Finally for u to remain bounded as $\tau \to \infty$ when $y = u_i + O(1)$ then we require

$$\zeta^{-1} \, \bar{G}(\zeta) \quad \text{bounded as} \quad \zeta \to \infty. \tag{2.28}$$

We recall from L, when considering parameter range (I), that we required a solution to (2.26), (2.27) which satisfied the boundary condition $\bar{G}(\zeta) \to \zeta$ as $\zeta \to \infty$. However, in this case we require a solution of (2.26), (2.27) which satisfies

$$\bar{G}(\zeta) \to 0^+ \quad \text{as} \quad \zeta \to \infty. \tag{2.29}$$

The boundary condition (2.29) can be developed to give

$$\bar{G}(\zeta) \sim D\,\zeta^{\frac{1}{4}} \, \exp\left(-\frac{2}{3\sqrt{3}}\zeta^{\frac{3}{2}}\right) \quad \text{as} \quad \zeta \to \infty, \tag{2.30}$$

8

where $D > 0$ is a constant. The leading order problem in this case is now complete, and is given by (2.26), (2.27) and (2.30). The boundary value problem (2.26)-(2.30) is both nonlinear and nonautonomous. A numerical study of initial-value problem (2.26), (2.30) using a shooting method (see [9] for details) reveals that a unique solution exists, which is oscillatory in $\zeta < 0$, being of the form (2.27) for $(-\zeta) \gg 1$ for each

$$D \in \left(0, \frac{3^{\frac{1}{4}}}{\sqrt{\pi}}\right).$$

We conclude that boundary value problem (2.26), (2.27) and (2.30) has a unique solution for each $D \in \left(0, \frac{3^{\frac{1}{4}}}{\sqrt{\pi}}\right)$. Moreover, for specified D, in the above range, then $\tilde{u}_\infty > 0$ and $\tilde{\theta}_\infty$ are fixed uniquely. The parameter D remains undetermined.

The remaining details of the large-τ asymptotic structure of the solution of **IBVP** follow, after minor modifications, those given in L and are summarized here for brevity.

Region **V(a)** $(-x) = O(\tau)$ as $\tau \to \infty$

$y = \frac{x}{\tau} = O(1)$ $\left(\in \left(u_i, \frac{u_i}{4}\right)\right)$ as $\tau \to \infty$ and ,

$$u(y, \tau) = u_i + \exp\left(-\frac{2}{3\sqrt{3}}(y - u_i)^{\frac{3}{2}}\tau - \frac{1}{2}\ln\tau + H(y) + o(1)\right)$$

as $\tau \to \infty$ with $y = O(1)$ $\left(\in \left(u_i, \frac{u_i}{4}\right)\right)$. $H(y) = O(1)$ is undetermined, with,

$$H(y) = \begin{cases} \frac{1}{4}\ln(y - u_i) + \ln D + o(1) & \text{as} \quad y \to u_i^+, \\ \ln H_c + o(1) & \text{as} \quad y \to \frac{u_i}{4}^- \end{cases}$$

where H_c is a constant.

Region **TR** $x = \frac{u_i}{4}\tau - \frac{1}{3(-u_i)^{\frac{1}{2}}}\ln\tau + O(1)$ as $\tau \to \infty$

$z = \left(x - \frac{u_i}{4}\tau + \frac{1}{3(-u_i)^{\frac{1}{2}}}\ln\tau\right) = O(1)$ as $\tau \to \infty$ and,

$$u(z, \tau) = u_i + \left[12(-u_i)e^{2x_c}e^{\sqrt{-u_i}z} + H_c e^{-\frac{1}{2}\sqrt{-u_i}z}\right]\tau^{-\frac{1}{3}}\exp\left[-\frac{1}{4}(-u_i)^{\frac{3}{2}}\tau\right]$$
$$+ o\left(\tau^{-\frac{1}{3}}\exp\left[-\frac{1}{4}(-u_i)^{\frac{3}{2}}\tau\right]\right)$$

as $\tau \to \infty$ with $z = O(1)$.

Region **V(b)** $(-x) = O(\tau)$ as $\tau \to \infty$

$y = \frac{x}{\tau} = O(1)$ $\left(\in \left(\frac{u_i}{4}, 0\right)\right)$ as $\tau \to \infty$ and,

$$u(y, \tau) = u_i + \exp\left(\sqrt{-u_i}y\tau + [2x_c + \ln 12(-u_i)]\right) + \hat{H}(y)\tau^{-\frac{1}{2}}\exp\left[-\frac{2}{3\sqrt{3}}(y - u_i)^{\frac{3}{2}}\tau\right]$$
$$+ o\left(\tau^{-\frac{1}{2}}\exp\left[-\frac{2}{3\sqrt{3}}(y - u_i)^{\frac{3}{2}}\tau\right]\right)$$

as $\tau \to \infty$ with $y = \frac{x}{\tau} = O(1)$ $\left(\in \left(\frac{u_i}{4}, 0\right)\right)$. $\hat{H}(y) = O(1)$ is undetermined, with

$$\hat{H}(y) = \begin{cases} H_c & \text{as} \quad y \to \frac{u_i}{4}^+, \\ c_0 y & \text{as} \quad y \to 0^-, \end{cases}$$
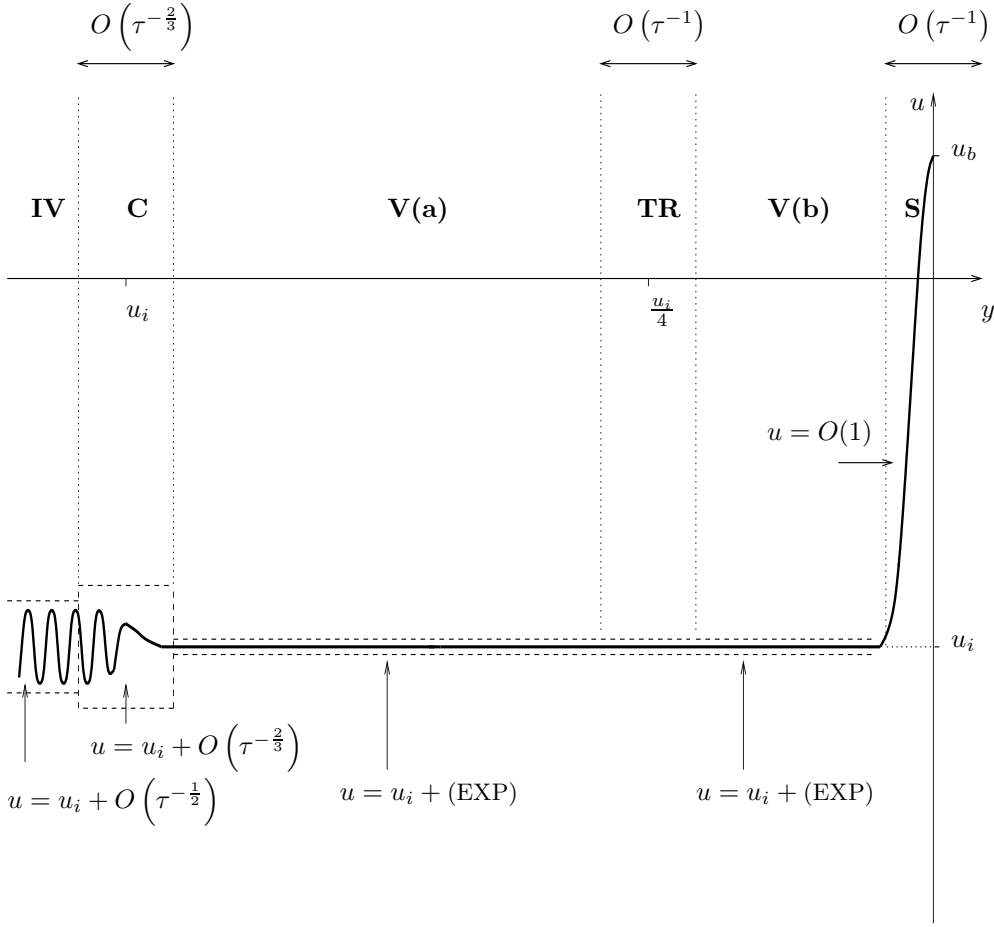
9

Figure 2: A schematic representation of the asymptotic structure of $u(y, \tau)$ in the (y, u) plane, as $\tau \to \infty$, when $0 < u_b < -2u_i$ and $|u_{bx}| = \frac{1}{\sqrt{3}}(u_b - u_i)(-u_b - 2u_i)^{\frac{1}{2}}$ (giving that $u_l = u_i$). Note the case when u_{bx} is positive is depicted in region **S**. Here (EXP) denotes terms exponentially small in τ as $\tau \to \infty$.

where c_0 is a constant.

Region **S** $\quad x = O(1) \ (\leq 0)$ as $\tau \to \infty$

$$u(x, \tau) = u_i - 3u_i \operatorname{sech}^2\left(\frac{\sqrt{-u_i}}{2}x + x_c\right) + O\left(\tau^{-\frac{3}{2}}\exp\left[-\frac{2}{3\sqrt{3}}(-u_i)^{\frac{3}{2}}\tau\right]\right)$$

as $\tau \to \infty$ with $x = O(1) \ (\leq 0)$, and where x_c is given by

$$x_c = \pm \operatorname{sech}^{-1}\left(\frac{u_b - u_i}{-3u_i}\right)^{\frac{1}{2}}$$

where the $-[+]$ sign is taken when $u_{bx} = \frac{1}{\sqrt{3}}(u_b - u_i)(-u_b - 2u_i)^{\frac{1}{2}}$ $[u_{bx} = -\frac{1}{\sqrt{3}}(u_b - u_i)(-u_b - 2u_i)^{\frac{1}{2}}]$ respectively. We note that the rate of convergence is exponential in τ as $\tau \to \infty$, being $O\left(\tau^{-\frac{3}{2}}\exp\left[-\frac{2}{3\sqrt{3}}(-u_i)^{\frac{3}{2}}\tau\right]\right)$.

This then completes the large-τ asymptotic structure of the solution to **IBVP** in case (II). A uniform approximation has been given through regions **III**, **IV**, **C**, **V(a)**, **TR**, **V(b)** and **S**. A sketch of the asymptotic structure of $u(x, \tau)$ as $\tau \to \infty$ is given in Figure 2.

10

2.3.2 Case (III) $0 < u_b < -2u_i$, $|u_{bx}| > \frac{1}{\sqrt{3}}(u_b - u_i)(-u_b - 2u_i)^{\frac{1}{2}}$

We recall in this case that the large-τ solution of **IBVP** exhibits the formation of a dispersive shock wave in $y \in \left(2u_l - u_i, \frac{2u_i}{3} + \frac{u_l}{3}\right)$, where $u_l < u_i$. As $y \to (2u_l - u_i)^+$ we approach the rear of the wave (the harmonic limit) and the solution approaches linear oscillations about u_i, with phase velocity v_p and wave number k, given by (1.18) and (1.19) respectively. A consideration of expansion (2.6) with (2.13)$_2$ indicates that we require $\alpha = k$, giving that $u_i - \alpha^2 = v_p$ and, via (2.14), that

$$y_T(k, u_i) = 2u_l - u_i.$$

Therefore, there exists a localized region, region **C**, within which the structure of the solution $g_0(y, k)$ changes from the the envelope solution (2.13)$_1$ to the linear solution (2.13)$_2$, which is consistent with the oscillatory behaviour at the rear of the dispersive shock wave (as $y \to (2u_l - u_i)^+$).

We begin in region **IV** where $y \in (-\infty, 2u_l - u_i)$. Here $g_0(y, \alpha)$ is given by (2.13)$_1$ (with $\alpha = k$) and following Section 2.3.1 we have that

$$u(y, \tau) = u_i + \frac{\bar{g}_3(y)}{\tau^{\frac{1}{2}}} \cos\left(\frac{2}{3\sqrt{3}}(u_i - y)^{\frac{3}{2}}\tau + g_2(y)\right) + o\left(\frac{1}{\tau^{\frac{1}{2}}}\right) \tag{2.31}$$

as $\tau \to \infty$, with $y \in (-\infty, 2u_l - u_i)$ and where the functions $\bar{g}_3(y)$ and $g_2(y)$ are as given in Section 2.3.1. As $y \to (2u_l - u_i)^-$ we move out of region **IV** into the localized connection region, region **C**, located at $y = (2u_l - u_i) + o(1)$. This localized region connects the oscillatory behaviour of region **IV** with the dispersive shock wave, the bulk of which is contained in region **DSW**, where $y \in \left(2u_l - u_i, \frac{2u_i}{3} + \frac{u_l}{3}\right)$ and $u = O(1)$. The approximate solution to **IBVP** in this region is given by (1.11) (with (1.12)).

To examine region **C** we introduce the scaled coordinate $\xi = \left(y - [2u_l - u_i]\right)\tau^{\frac{1}{2}}$, where $\xi = O(1)$ as $\tau \to \infty$, and write (as suggested by (2.31))

$$u(\xi, \tau) = u_i + \left[\hat{F}(\xi) + o(1)\right]\left\{e^{iG(\xi,\tau)} + e^{-iG(\eta,\tau)}\right\} \tag{2.32}$$

with

$$G(\xi, \tau) = -2A^3\tau + A\xi\tau^{\frac{1}{2}} + \hat{G}(\xi) + o(1), \tag{2.33}$$

as $\tau \to \infty$, where

$$A = -\sqrt{\frac{2(u_i - u_l)}{3}} \quad (= -k)$$

and $\hat{F}(\xi)(> 0)$, $\hat{G}(\xi)$ are functions to be determined. We recall in this case that $u_i - u_l > 0$. On substitution of (2.32), (2.33) into equation (1.1) (when written in terms of ξ and τ), we obtain

$$3A\,\hat{F}\hat{G}_{\xi\xi} + 6A\,\hat{F}_\xi\hat{G}_\xi + \frac{\xi}{2}\hat{F}_\xi = 0, \tag{2.34}$$

$$-3A\,\hat{F}_{\xi\xi} + 3A\,\hat{F}\hat{G}_\xi^2 + \frac{\xi}{2}\hat{F}\hat{G}_\xi = 0, \tag{2.35}$$

where $-\infty < \xi < \infty$. Now, matching expansion (2.31) $\left(y \to (2u_l - u_i)^-\right)$ with expansion (2.32) ($\xi \to -\infty$) requires that,

$$\bar{g}_3(y) \sim \frac{D}{([2u_l - u_i] - y)}, \quad g_2(y) \sim c_1,$$

as $y \to (2u_l - u_i)^-$, where $D\,(> 0)$ and c_1 are unknown constants. Hence, equations (2.34) and (2.35) are to be solved subject to the matching conditions

11

	A			
D	-0.5000	-1.0000	-1.5000	-2.0000
0.1000	0.1446...	0.1023...	0.0835...	0.0723...
1.0000	1.446...	1.0227...	0.835...	0.723...
10.0000	14.46...	10.227...	8.3499...	7.23...

Table 1: Numerical estimates of F_∞ $\left(\approx \hat{F}(500) \right)$

	A			
D	-0.5000	-1.0000	-1.5000	-2.0000
0.1000	$-0.785...$	$-0.785...$	$-0.785...$	$-0.785...$
1.0000	$-0.785...$	$-0.785...$	$-0.785...$	$-0.785...$
10.0000	$-0.785...$	$-0.785...$	$-0.785...$	$-0.785...$

Table 2: Numerical estimates of G_∞ $\left(\approx \hat{G}(500) \right)$

$$\hat{F}(\xi) \sim \begin{cases} F_\infty & \text{as} \quad \xi \to \infty, \\ D\,(-\xi)^{-1} & \text{as} \quad \xi \to -\infty, \end{cases} \tag{2.36}$$

and

$$\hat{G}(\xi) \sim \begin{cases} G_\infty & \text{as} \quad \xi \to \infty, \\ -\frac{\xi^2}{12A} & \text{as} \quad \xi \to -\infty, \end{cases} \tag{2.37}$$

where the constants F_∞ and G_∞ are unknown at this stage. Boundary value problem (2.33),(2.34),(2.36) and (2.37) is a nonlinear nonautonomous coupled system. We observe from equations (2.34) and (2.35) that

$$\hat{F}_\xi^2 + \hat{F}^2\,\hat{G}_\xi^2 = \mathcal{C}, \tag{2.38}$$

where $\mathcal{C}$ is a positive constant. Consideration of boundary conditions $(2.36)_2$ and $(2.37)_2$ gives that

$$\mathcal{C} = \left(\frac{D}{6A} \right)^2,$$

and we further note that boundary conditions $(2.36)_1$ and $(2.37)_1$ can be developed to give

$$\hat{F}(\xi) = F_\infty + O\left(\frac{1}{\xi}\,\cos\left[\frac{\xi^2}{12|A|} + \dots \right] \right) \tag{2.39}$$

and

$$\hat{G}(\xi) = G_\infty + O\left(\frac{1}{\xi}\,\sin\left[\frac{\xi^2}{12|A|} + \dots \right] \right) \tag{2.40}$$

as $\xi \to \infty$.

A numerical study of initial-value problem (2.34), (2.35), $(2.36)_2$, $(2.37)_2$ using a shooting method reveals, for given values of u_i and u_l, that a unique solution exists for each $D > 0$. We note that the initial-value problem was solved by truncating the domain to $\xi \in (-L, L)$, where $L = 500$ was taken in what follows. Graphs of $\hat{F}(\xi)$ and $\hat{G}(\xi)$ against ξ illustrating a typical solution of this initial value problem when $A = -1$ and $D = 20$, are shown in Figure 3. We have for $A = -1$ and $D = 20$ the following numerical estimates $F_\infty \approx 20.4$ and $G_\infty \approx -0.785$. Although F_∞ and G_∞ remain undetermined in this analysis numerical solutions of the initial-value problem for values of $A = -\frac{1}{2}, -1, -\frac{3}{2}$ and -2, and $D = 10^{-1}, 1$ and 10, indicate that F_∞ is an affine function of D, for fixed A. Further, G_∞ is independent of both A and D, with $G_\infty \approx -0.785$. The results are shown in Tables 1 and 2.

We conjecture that there exists a unique $D > 0$, say $D = D^*$, for given values of u_i and u_l, for which boundary value problem (2.34), (2.35), (2.36) and (2.37) has a unique solution.

As $y \to y_R^-$ (where $y_R = \frac{2u_i}{3} + \frac{u_l}{3}$) we move out of region **DSW** into region **S1**, where $y = y_R + O\left(\tau^{-1}\right)$ as $\tau \to \infty$. To examine region **S1** we introduce the scaled coordinate $\eta = (y - y_R)\tau$, and write

$$u(\eta, \tau) = \left(u_l + \bar{u}(\eta) \right) + o(1) \tag{2.41}$$

as $\tau \to \infty$ with $\eta = O(1)$. On substituting (2.41) into equation (1.1) (when written in terms of η and τ) we obtain

$$\bar{u}_{\eta\eta} + \bar{u}\bar{u}_\eta + (u_l - y_R)\,\bar{u}_\eta = 0, \quad -\infty < \eta < \infty, \tag{2.42}$$

$$\bar{u}(\eta) \to 0^+ \quad \text{as} \quad \eta \to \infty, \tag{2.43}$$

$$\bar{u}(\eta) \quad \text{bounded as} \quad \eta \to -\infty. \tag{2.44}$$

We can integrate (2.42) once, and use the condition as $\eta \to \infty$, to obtain

$$\bar{u}_{\eta\eta} + \frac{1}{2}\bar{u}^2 - (y_R - u_l)\,\bar{u} = 0, \quad -\infty < \eta < \infty, \tag{2.45}$$

in place of (2.42). The solution to boundary value problem (2.45), (2.43) and (2.44) is readily obtained as

$$\bar{u}(\eta) = 2(u_i - u_l)\operatorname{sech}^2\left(\sqrt{\frac{u_i - u_l}{6}}\,\eta + \phi_0 \right), \quad -\infty < \eta < \infty, \tag{2.46}$$

where ϕ_0 is a constant. Solution (2.46) represents a soliton. Therefore, in region **S1** we have that

$$u(\eta, \tau) = u_l + 2(u_i - u_l)\operatorname{sech}^2\left(\sqrt{\frac{u_i - u_l}{6}}\,\eta + \phi_0 \right) + o(1) \tag{2.47}$$

as $\tau \to \infty$ with $\eta = O(1)$, which is in agreement with (1.17). As $\eta \to \infty$ we move out of region **S1** into region **V** where $y = O(1)$ ($\in (y_R, 0)$). We now examine the form of (2.47) for $\eta \gg 1$ (as we move into region **V**). From (2.47) we have

$$u(\eta, \tau) \sim u_l + \mathcal{A}\,\exp\left(-\sqrt{\frac{2}{3}(u_i - u_l)}\,\eta \right) \tag{2.48}$$

with $\eta \gg 1$, where $\mathcal{A} = 8(u_i - u_l)e^{-2\phi_0}$ (> 0). When written in terms of y, (2.48) becomes

$$u(\eta, \tau) \sim u_l + \mathcal{A}\,\exp\left(-\sqrt{\frac{2}{3}(u_i - u_l)}\left(y - \left[\frac{2u_i}{3} + \frac{u_l}{3} \right] \right) \right). \tag{2.49}$$

Thus, we must look for an expansion in region **V** in the form

$$u(y, \tau) = u_l + e^{-\tau H(y, \tau)}, \tag{2.50}$$

where

$$H(y, \tau) = h_0(y) + h_1(y)\frac{1}{\tau} + o\left(\frac{1}{\tau}\right) \quad \text{as} \quad \tau \to \infty, \tag{2.51}$$

with $y = O(1)$ ($\in (y_R, 0)$) as $\tau \to \infty$. Substitution of (2.50), (2.51) into equation (1.1) (when written in terms of y and τ) gives on solving at each order in turn and matching to expansion (2.49) as $y \to y_R^+$ that

$$u(y, \tau) = u_l + \exp\left(-\sqrt{\frac{2}{3}(u_i - u_l)}\left(y - \left[\frac{2u_i}{3} + \frac{u_l}{3} \right] \right) + \ln\mathcal{A} + o(1) \right) \tag{2.52}$$
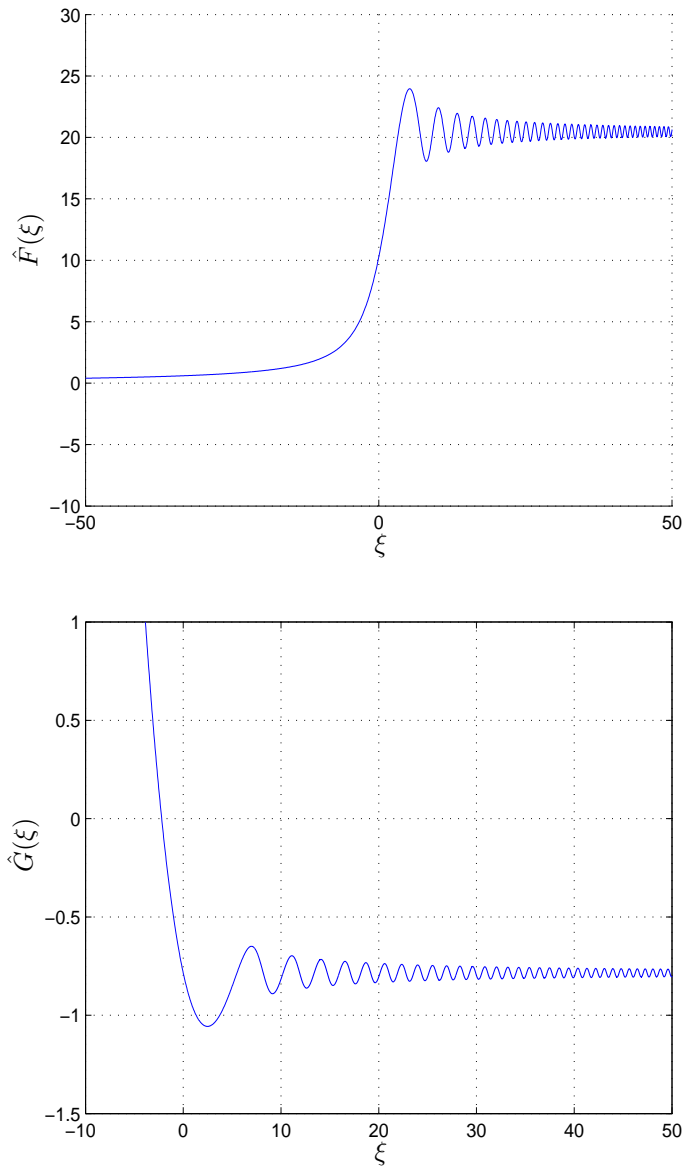
Figure 3: Graphs of $\hat{F}(\xi)$ and $\hat{G}(\xi)$ against ξ. Here $F_\infty \approx 20.4$ and $G_\infty \approx -0.785$.

as $\tau \to \infty$ with $y = O(1)$ $(\in (y_R, 0))$.

At this stage we recall that as in Section 2.3.1, the solution to **IBVP** when $x = O(1) (\le 0)$ in region **S**, which satisfies boundary conditions (1.3) and (1.4), is given by

$$u(x, \tau) = u_l - 3u_l \operatorname{sech}^2 \left(\frac{\sqrt{-u_l}}{2} x + x_c \right) + o(1) \qquad (2.53)$$

as $\tau \to \infty$ with $x = O(1) (\le 0)$, where

$$x_c = \pm \operatorname{sech}^{-1} \left(\frac{u_b - u_l}{-3u_l} \right)^{\frac{1}{2}}. \qquad (2.54)$$

The $-[+]$ sign in (2.54) is taken when u_{bx} is positive [negative] respectively. The correction to expansion (2.53) will be determined at a later stage in this analysis. From (2.53) we observe that

$$u(x, \tau) \sim u_l + \mathcal{B} \exp \left(\sqrt{-u_l}\, x \right) + \dots \qquad (2.55)$$

for $(-x) \gg 1$, where $\mathcal{B} = -12u_l e^{2x_c}$.

Clearly, matching expansion (2.52) (as $y \to 0^-$) to expansion (2.53) (as $x \to -\infty$) fails, and we conclude that region **V** must be replaced by three regions: region **V(a)** $\left(y \in (y_R, y_t) \right)$, region **TR** (transition region), and region **V(b)** $\left(y \in (y_t, 0) \right)$, where y_t is to be determined. It is readily established that:

Region **V(a)**

$$u(y, \tau) = u_l + \exp \left(-\sqrt{\frac{2}{3}(u_i - u_l)} \left(y - \left[\frac{2u_i}{3} + \frac{u_l}{3} \right] \right) \tau + \ln \mathcal{A} + o(1) \right) \qquad (2.56)$$

as $\tau \to \infty$ with $y = O(1)$ $(\in (y_R, y_t))$.

Region **V(b)**

$$u(y, \tau) = u_l + \exp \left(\sqrt{-u_l}\, y\tau + \ln \mathcal{B} + o(1) \right) \qquad (2.57)$$

as $\tau \to \infty$ with $y = O(1)$ $(\in (y_t, 0))$.

We now examine the transition region, region **TR**. An examination of expansion (2.56) (as $y \to y_t^-$) and expansion (2.57) (as $y \to y_t^+$) reveals that in this region $y = y_t + O\left(\tau^{-1} \right)$ as $\tau \to \infty$, where

$$y_t = \frac{y_R \sqrt{\frac{2}{3}(u_i - u_l)}}{\sqrt{\frac{2}{3}(u_i - u_l)} + \sqrt{-u_l}} \quad (< 0). \qquad (2.58)$$

To examine region **TR** we introduce the scaled coordinate $z = (y - y_t)\tau$, where $z = O(1)$ as $\tau \to \infty$, and expand as

$$u(z, \tau) = u_l + \left(F(z) + o(1) \right) \exp \left(y_t \sqrt{-u_l}\tau \right) \qquad (2.59)$$

as $\tau \to \infty$ with $z = O(1)$. On substitution of (2.59) into equation (1.1) (when written in terms of z and τ) we obtain at leading order

$$F_{zzz} + (u_l - y_t) F_z + y_t \sqrt{-u_l}\, F = 0, \quad -\infty < z < \infty. \qquad (2.60)$$

Equation (2.60) is to solved subject to the boundary conditions

$$F(z) \sim \begin{cases} \mathcal{A} \exp \left(-\sqrt{\frac{2}{3}(u_i - u_l)}\, z \right) & \text{as} \quad z \to -\infty, \\[2mm] \mathcal{B} \exp \left(\sqrt{-u_l}\, z \right) & \text{as} \quad z \to \infty. \end{cases} \qquad (2.61)$$

Conditions (2.61) are the matching conditions with regions **V(a)** and **V(b)** respectively. The solution of (2.60) and (2.61) is readily obtained as

$$F(z) = \mathcal{A} \exp\left(-\sqrt{\frac{2}{3}(u_i - u_l)}\, z\right) + \mathcal{B} \exp\left(\sqrt{-u_l}\, z\right), \quad -\infty < z < \infty. \quad (2.62)$$

Expansion (2.57) in region **V(b)** can now be developed to give

$$u(y, \tau) = u_l + \exp\left(\sqrt{-u_l}\, y\tau + \ln \mathcal{B}\right) + \exp\left(-\sqrt{\frac{2}{3}(u_i - u_l)}\,(y - y_R)\tau + \ln \mathcal{A}\right)$$
$$+ o\left(\exp\left(-\sqrt{\frac{2}{3}(u_i - u_l)}\,(y - y_R)\tau\right)\right) \quad (2.63)$$

as $\tau \to \infty$ with $y = O(1)\,(\in (y_t, 0))$. On examining expansion (2.63) in region **V(b)** (as $y \to 0^-$), we obtain from (2.63), when written in terms of x, that

$$u(x, \tau) \sim u_l + \mathcal{B} \exp\left(\sqrt{-u_l}\, x\right) + \mathcal{A} \exp\left(-\sqrt{\frac{2}{3}(u_i - u_l)}\, x\right) \exp\left(\sqrt{\frac{2}{3}(u_i - u_l)}\, y_R \tau\right)$$
$$(2.64)$$

as $\tau \to \infty$ with $(-x) \gg 1$. On examining (2.64) we determine that the correction to expansion (2.53) of region **S** is $O\left(\exp\left(\sqrt{\frac{2}{3}(u_i - u_l)}\, y_R \tau\right)\right)$ as $\tau \to \infty$.

Hence, in region **S** we expand as

$$u(x, \tau) = u_s(x) + u_1(x) \exp\left(\sqrt{\frac{2}{3}(u_i - u_l)}\, y_R \tau\right) + o\left[\exp\left(\sqrt{\frac{2}{3}(u_i - u_l)}\, y_R \tau\right)\right]$$
$$(2.65)$$

as $\tau \to \infty$ with $x = O(1)\,(\leq 0)$, and where $u_s(x)$ is given by (1.5). On substitution of (2.65) into equation (1.1) we obtain the equation for $u_1(x)$ as

$$u_1''' + u_s u_1' + \left(u_s' + \sqrt{\frac{2}{3}(u_i - u_l)}\, y_R\right) u_1 = 0, \quad x \leq 0. \quad (2.66)$$

On recalling that

$$u_s(x) \sim u_l + \mathcal{B} \exp\left(\sqrt{-u_l}\, x\right)$$

as $x \to -\infty$, we have, via (2.66), that

$$u_1(x) \sim \mathcal{D} \exp\left(-\sqrt{\frac{2}{3}(u_i - u_l)}\, x\right) \quad (2.67)$$

as $x \to -\infty$, where $\mathcal{D}$ is a constant to be determined. Matching expansion (2.65) (as $x \to -\infty$) with expansion (2.64) up to exponentially small terms of

$$O\left(\exp\left(\sqrt{\frac{2}{3}(u_i - u_l)}\, y_R \tau\right)\right)$$

as $\tau \to \infty$, requires that

$$\mathcal{D} = \mathcal{A}.$$

Finally, we have in region **S** that

$$u(x, \tau) = u_i - 3u_i \,\mathrm{sech}^2\left(\frac{\sqrt{-u_i}}{2}x + x_c\right) + O\left(\exp\left[-\left(\frac{2}{3}\right)^{\frac{3}{2}}(u_i - u_l)^{\frac{1}{2}}\left(-u_i - \frac{u_l}{2}\right)\tau\right]\right)$$
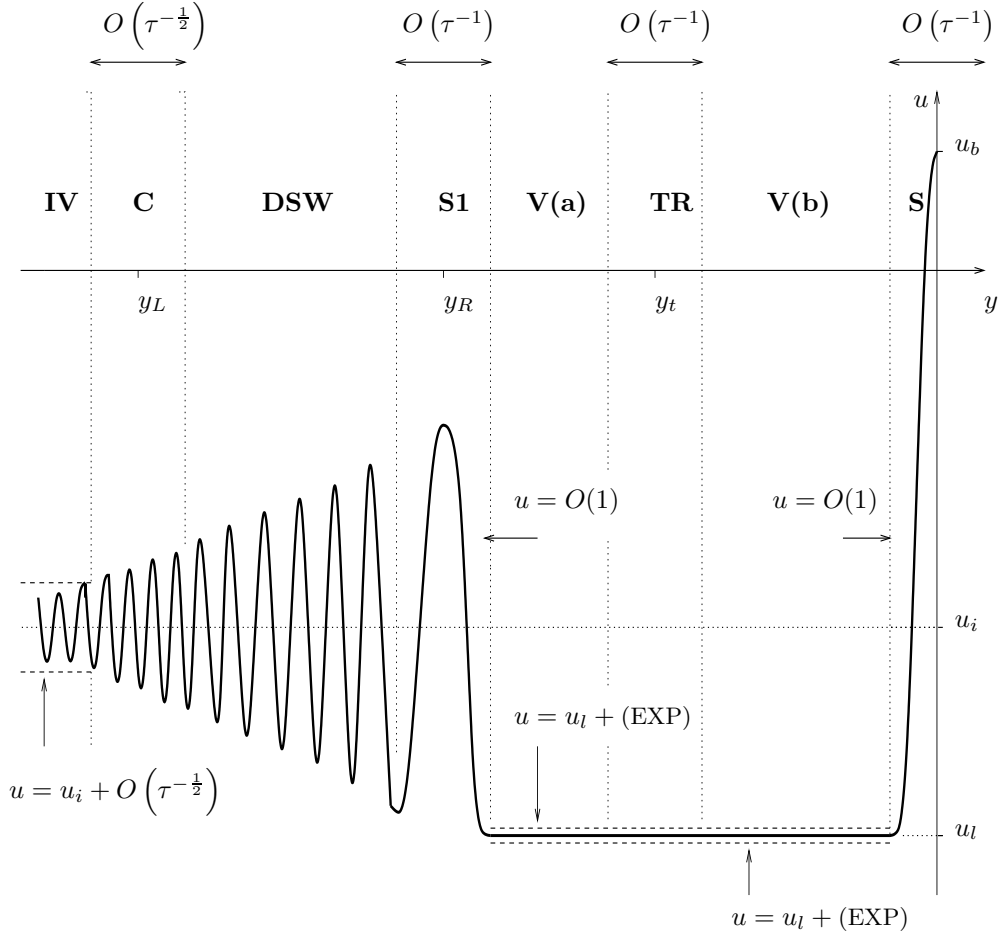$$(2.68)$$

16

Figure 4: A schematic representation of the asymptotic structure of $u(y, \tau)$ in the (y, u) plane, as $\tau \to \infty$, when $0 < u_b < -2u_i$ and $|u_{bx}| > \frac{1}{\sqrt{3}}(u_b - u_i)(-u_b - 2u_i)^{\frac{1}{2}}$ (where $u_l < u_i$). Note the case when u_{bx} is positive is depicted in region **S**. Here $y_L = 2u_l - u_i$, $y_R = \frac{2u_i}{3} + \frac{u_l}{3}$, $y_t = \frac{y_R \sqrt{\frac{2}{3}(u_i - u_l)}}{\sqrt{\frac{2}{3}(u_i - u_l)} + \sqrt{-u_l}}$ and (EXP) denotes terms exponentially small in τ as $\tau \to \infty$. We note that $y_L \to u_i^-$ and $y_R \to u_i^-$ as $u_l \to u_i^-$.

as $\tau \to \infty$ with $x = O(1)$ (≤ 0), and where x_c is given by (2.54). We note that the rate of convergence is exponential in τ as $\tau \to \infty$, being

$$O\left(\exp\left[-\left(\frac{2}{3}\right)^{\frac{3}{2}}(u_i - u_l)^{\frac{1}{2}}\left(-u_i - \frac{u_l}{2}\right)\tau\right]\right).$$

This then completes the large-τ asymptotic structure of the solution to **IBVP** in case (III). A uniform approximation has been given through regions **III**, **IV**, **C**, **DSW**, **S1**, **V(a)**, **TR**, **V(b)** and **S**. A sketch of the asymptotic structure of $u(x, \tau)$ as $\tau \to \infty$ is given in Figure 4.

3   Numerical results

In this section we perform representative numerical solutions to **IBVP** for comparision to the asymptotic results presented in Section 2. To achieve this we use essentially the same finite-difference and explicit Runge-Kutta ('RK4') algorithm as that used by Marchant and Smyth in [14]. A description of this scheme is given in Appendix A.

17

The results given below correspond to solving over the spatial interval $(L, 0)$ using M equal width intervals, and over the time interval $(0, T)$ using N equal width time steps. We define the step sizes $\Delta x = -L/M$ and $\Delta \tau = T/N$, and set $x_j = -j \, \Delta x$ and $\tau_i = i \, \Delta \tau$ for $j \in \{0, 1, 2, \ldots, M\}$ and $i \in \{0, 1, 2, \ldots, N\}$. In each of the cases shown we set $T = 70$ and $L = -700$, although the x axis in the plots has in two cases been shortened in order to better display the features of interest.
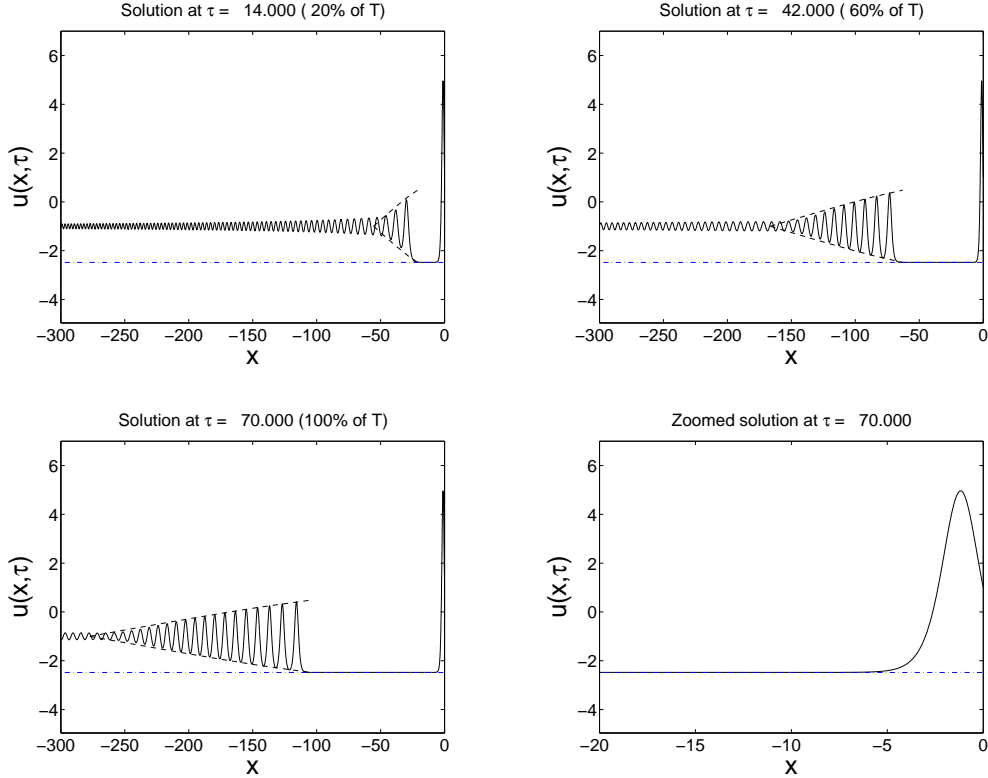

Figure 5: Numerical solution of **IBVP** when $u_i = -1$, $u_b = 1$ and $u_{bx} = -4$ for $\tau = 14, 42, 70$, where $(L, 0) = (-700, 0)$ and $(0, T) = (0, 70)$. We note that $u_l \approx -2.4808$.

In their numerical simulations Marchant and Smyth use $\Delta x = 0.1$ and $\Delta \tau = 0.001$ and verified stability and accuracy. We found it necessary to use the next natural finer approximation, $\Delta x = 0.05$ and $\Delta \tau = 0.0001$, because we had difficulty in resolving the vertical position of the platform in front of the shock. Since we are building on Marchant and Smyth's discrete scheme we did not consider it necessary to implement any form of error or step size control.

We first consider Figures 5 and 6 which show, for increasing time, the development of the solution $u(x, \tau)$ of **IBVP** for two sets of the parameter values u_i, u_b and u_{bx} corresponding to case (III) of Section 2. In these figures the horizontal dot-dash line denotes u_l, whereas the dashed line denotes the predicted wave envelope. In both figures the development of the predicted dispersive shock can clearly be seen, and we note the excellent agreement between the numerical solutions presented and the predicted wave envelopes. Further, in both figures we note the rapid (exponential) convergence of the solution to the steady state profile $u_s(x)$, given by (1.5), again in line with the results of Section 2. Figure 5 shows the development of the solution to **IBVP** for $u_i = -1$, $u_b = 1$ and $u_{bx} = -4$ for $\tau = 14, 42, 70$. The development of the predicted dispersive shock wave connecting $u = -1$ to $u = u_l$ (≈ -2.4808) can clearly be seen. Figure 6 shows the development of the solution of **IBVP** for $u_i = -2$, $u_b = 1$
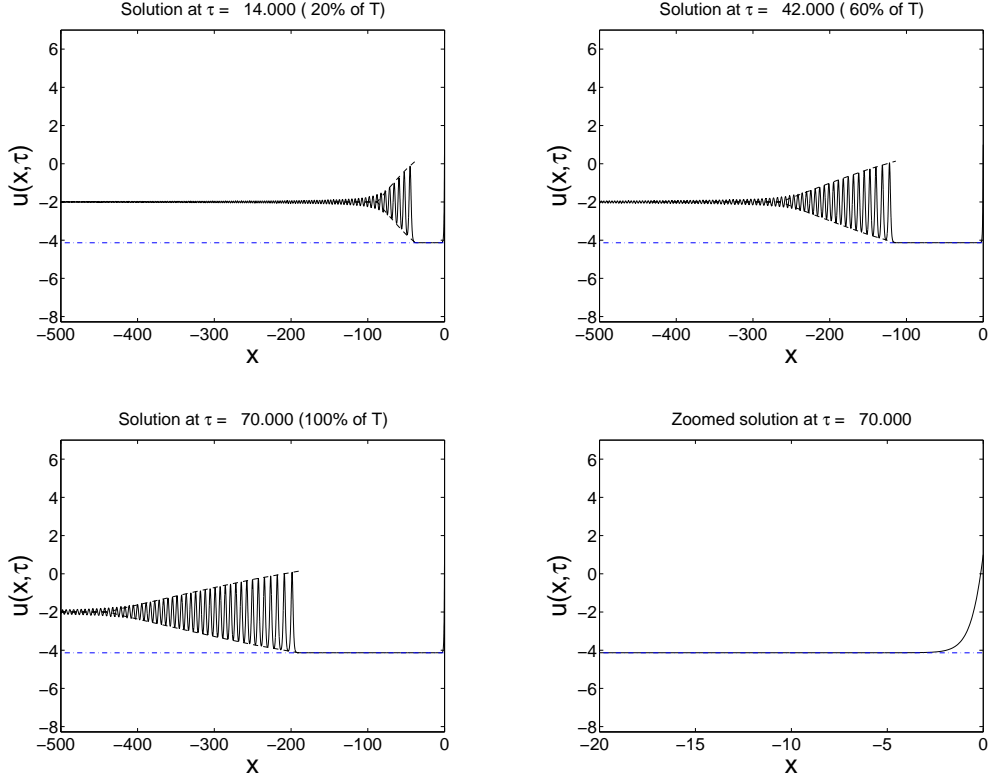
18

Figure 6: Numerical solution of **IBVP** when $u_i = -2$, $u_b = 1$ and $u_{bx} = 8$ for $\tau = 14, 42, 70$, where $(L, 0) = (-700, 0)$ and $(0, T) = (0, 70)$. We note that $u_l \approx -4.1374$.

and $u_{bx} = 8$ for $\tau = 14, 42, 70$. Again the development of the predicted dispersive shock wave can clearly be been seen, in this case connecting $u = -2$ to $u = u_l (\approx -4.1374)$. In both Figures 5 and 6 a zoomed plot of $u(x, 70)$ against x, for $x \in (-20, 0)$, is given which illustrates clearly the development of the steady state profile $u_s(x)$.

Finally, Figure 7 shows, for increasing time, the development of the solution $u(x, \tau)$ of **IBVP** for $u_i = -1$, $u_b = 4$ and $u_{bx} = -12$ for $\tau = 14, 42, 70$. Here $u_b > -2u_i$ in contrast to the previous two figures where $0 < u_b < -2u_i$. However, we recall that the analysis presented in Section 2 for case (III) can be readily extended to consider the large-τ solution to **IBVP** when $u_i < 0$ and with boundary values u_b and u_{bx} in the ranges $u_b > -2u_i$ and $u_{bx} \in (-\infty, \infty)$. Again we clearly see the development of the predicted dispersive shock wave connecting, in this case, $u = -1$ to $u = u_l (\approx -4.7934)$. A zoomed plot of $u(x, 70)$ against x, for $x \in (-20, 0)$, is given which again illustrates clearly the development of the steady state profile $u_s(x)$.

4   Discussion

In this paper we have obtained, via the method of matched asymptotic coordinate expansions, the uniform asymptotic structure of the large-τ solution to **IBVP** when $u_i < 0$ and with boundary values u_b and u_{bx} in the ranges (II) and (III). The results presented here are complementary to those reported in L, for boundary values in range (I). The large-τ structure of the solution to **IBVP** was obtained by careful consideration of the asymptotic structures as $\tau \to 0$ $(-\infty < x \le 0)$ and $x \to -\infty$ $(\tau \ge O(1))$. Schematic representations of the structure of the large-τ solution of **IBVP** in cases (II) and (III) are given in Figures 2 and 4 respectively. In Section 3 we

have presented numerical solutions to initial-boundary value problem **IBVP** in case (II), which support and illustrate the detailed analysis developed in Section 2.

It has been established that the solution, $u(x,\tau)$, to **IBVP** for $x = O(1)\,(\leq 0)$ in cases (II) and (III) is the steady state solution $u_s(x)$ (given by (1.5)), with the rate of convergence being exponentially small in τ, as $\tau \to \infty$. Specifically, in region **S**, we have that

$$u(x,\tau) = u_s(x) + \begin{cases} O\left(\tau^{-\frac{3}{2}} \exp\left[-\frac{2}{3\sqrt{3}}(-u_i)^{\frac{1}{2}}\tau\right]\right), & \text{Case (II)} \quad (u_l = u_i) \\[2ex] O\left(\exp\left[-\left(\frac{2}{3}\right)^{\frac{3}{2}}(u_i - u_l)^{\frac{1}{2}}\left(-u_i - \frac{u_l}{2}\right)\tau\right]\right), & \text{Case (III)} \quad (u_l < u_i) \end{cases}$$

as $\tau \to \infty$ with $x = O(1)\,(\leq 0)$, and where u_l is given by (1.6) (with (1.7)). In case (II) [(III)] the solution of **IBVP**, through regions **V(a)**-**V(b)** where $(-x) = O(\tau)$ as $\tau \to \infty$, is given at leading order by the constant value u_i [u_l] respectively. In both cases region **IV** allows for the transfer of information from the far field $(-y) \gg 1$ [that is, $(-x) \gg \tau$] to the near field $(y = O(1))$. Within this region the solution to **IBVP** is oscillatory, oscillating about u_i, with $u = u_i + O\left(\tau^{-\frac{1}{2}}\right)$ as $\tau \to \infty$. In case (II), region **V(a)** is connected to region **IV** by a localized connection region, region **C**, located at $y = u_i + O\left(\tau^{-\frac{2}{3}}\right)$ $\left[\text{that is, } x = u_i\tau + O\left(\tau^{\frac{1}{3}}\right)\right]$ as $\tau \to \infty$, where $u = u_i + O\left(\tau^{-\frac{2}{3}}\right)$. However, in case (III) $(u_l < u_i)$, regions **IV** and **V(a)** are connected by a dispersive shock wave, which allows for the adjustment in the value of u from the wave front (where $u \sim u_l$) to the rear of the wave (where $u \sim u_i$). The bulk of this dispersive shock wave is contained in region **DSW**, while the localized connection regions **C** and
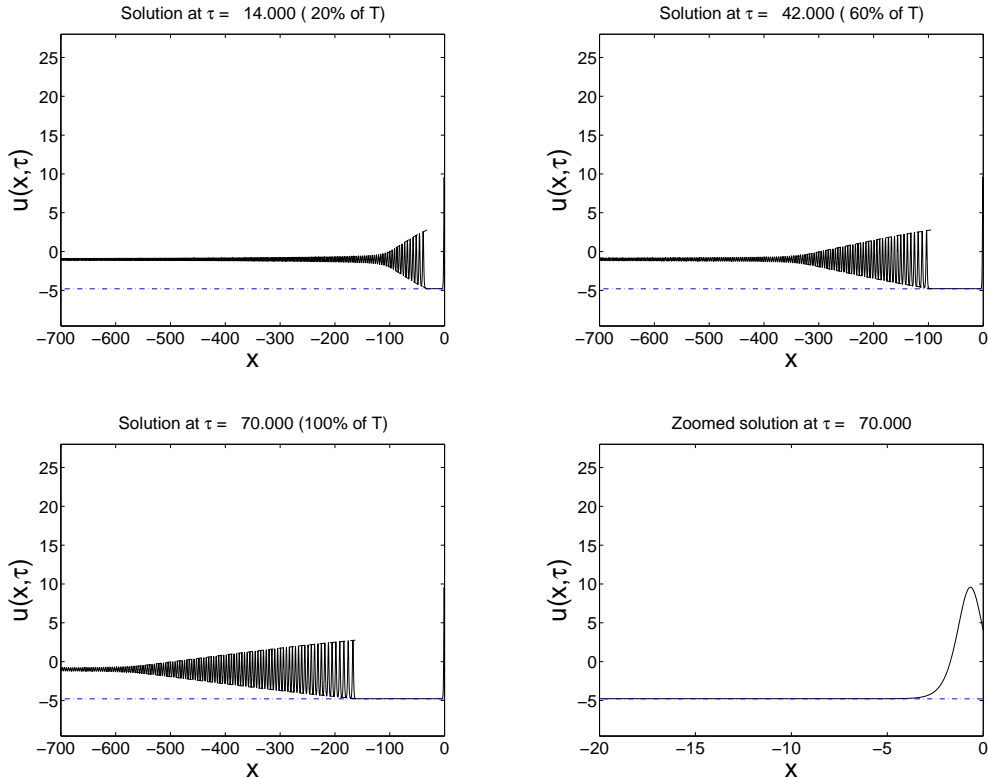

Figure 7: Numerical solution of **IBVP** when $u_i = -1$, $u_b = 4$ and $u_{bx} = -12$ for $\tau = 14, 42, 70$, where $(L, 0) = (-700, 0)$ and $(0, T) = (0, 70)$. We note that $u_l \approx -4.7934$.

20

S1 are located at $y_L = 2u_l - u_i$ and $y_R = \frac{2u_i}{3} + \frac{u_l}{3}$ respectively. This dispersive shock wave is given approximately by (1.11) (with (1.12)). We note that $y_L \to u_i^-$ and $y_R \to u_i^-$ as $u_l \to u_i^-$ [that is, as we approach case (II)]. We further note the excellent agreement between the numerical solutions presented in Section 3 and the predicted wave envelope u_e (given by (1.16)) of the dispersive shock wave.

We conclude by noting that the analysis presented in this paper can be readily extended to consider the large-τ solution to **IBVP** when $u_i < 0$ and with boundary values u_b and u_{bx} in the ranges $u_b \geq -2u_i$ and $u_{bx} \in (-\infty, \infty)$. In particular, when

(i) $(u_b = -2u_i, u_{bx} = 0)$
    The large-τ structure of the solution of **IBVP** follows that given for case (II).

(ii) $(u_b > -2u_i, u_{bx} \in (-\infty, \infty))$ or $(u_b = -2u_i, u_{bx} \neq 0)$
    The large-τ structure of the solution of **IBVP** follows that given for case (III).

This extension then gives a complete description of the large-τ solution of **IBVP** for $u_i < 0$, $u_b > 0$ and $u_{bx} \in (-\infty, \infty)$.

It should be noted that the approach presented can be applied, after minor modification, to examine the large-time solution of **IBVP** when $u_i > 0$.

A   Appendix: the numerical scheme for the initial boundary-value problem

Denoting the semidiscrete approximation resulting from spatial discretisation by $v_j(\tau) \approx u(x_j, \tau)$ a finite difference approximation to the Korteweg-de Vries equation on the negative quarter plane can then be written for $j \geqslant 2$ as,

$$\frac{dv_j}{d\tau} = \frac{(v_{j+1} - v_{j-1})v_j}{2\,\Delta x} + \frac{v_{j+2} - 2v_{j+1} + 2v_{j-1} - v_{j-2}}{2\,\Delta x^3}$$
$$\text{with } v_j(0) = u_i.$$

(Note that since the positioning subscripts appear only on the approximate solution, v, there should be no confusion caused by the subscripts in u_i, u_b and u_{bx}.) Also, when $j = 0$ we get $dv_0/d\tau = 0$ for all $\tau > 0$ since $v_0(\tau) = u_b$. In the discrete scheme we set $v_0(0) = u_b$ also even though this may not be consistent with the initial datum.

We treat the case $j = 1$ a little differently to Marchant and Smyth, [14], by introducing a 'ghost point' at $x_{-1} = \Delta x$. Then, since $u_\tau(0, \tau) = 0$ we get $u_{xxx}(0, \tau) = -u(0, \tau)u_x(0, \tau) = -u_b u_{bx}$ and it follows then from Taylor's series that $u(\Delta x, \tau) = u(-\Delta x, \tau) + 2\Delta x\, u_{bx} - 3^{-1}\Delta x^3 u_b u_{bx} + O(\Delta x^5)$. Dropping the error term to form the approximation and introducing this into the finite difference formula given above for $j \geqslant 2$ but, now, for $j = 1$ also, results in

$$\frac{dv_1}{d\tau} = \frac{(v_2 - v_0)v_1}{2\,\Delta x} + \frac{v_3 - 2v_2 - v_1 + 2v_0}{2\,\Delta x^3} - \frac{(6 - \Delta x^2\, u_b)u_{bx}}{6\Delta x^2}$$
$$\text{with } v_1(0) = u_i.$$

These approximations are all of order $O(\Delta x^2)$ and writing $\boldsymbol{v} = (v_0, v_1, \ldots)^T$ we have arrived at the autonomous system of ordinary differential equations $\dot{\boldsymbol{v}} = \boldsymbol{f}(\boldsymbol{v})$ with $\boldsymbol{v}(0)$ given.

This system is approximated with the fourth order Runge-Kutta method defined by $\boldsymbol{v}^i = \boldsymbol{v}^{i-1} + 6^{-1}\Delta\tau(\boldsymbol{k}_1 + 2\boldsymbol{k}_2 + 2\boldsymbol{k}_3 + \boldsymbol{k}_4)$ where $\boldsymbol{k}_n = \boldsymbol{f}(\boldsymbol{v}^{i-1} + \alpha_n\Delta\tau\boldsymbol{k}_{n-1})$ for $(\alpha_1, \ldots, \alpha_4) = (0, \frac{1}{2}, \frac{1}{2}, 1)$ and with $\boldsymbol{k}_0 := 0$. Here, of course, $\boldsymbol{v}^i$ is the approximation to $\boldsymbol{v}(t_i)$ and $\boldsymbol{v}^0 = \boldsymbol{v}(0)$. The error per step of this method is $O(\Delta\tau^5)$ and so the accumulated error is $O(\Delta\tau^4)$. The well-known downside of this scheme is that it is only conditionally stable requiring, in this case, $\Delta\tau \leqslant C\Delta x^3$.

Our numerical simulations show computed solutions over $(L, 0)$ at certain discrete times $\tau \leqslant T$. To accomplish this we started at $\tau = 0$ with a grid consisting of $\widehat{M} = pM + 2N$ intervals extending over $(\widehat{L}, 0)$. Here $\widehat{L} = \widehat{M} \Delta x$ and $p \geqslant 1$ is a 'padding constant'. The idea is to explicitly step forward from a set of intervals that contracts by two grid points at each time step and so it follows that after m time steps there will be only $pM + 2N - 2m$ intervals carrying data at τ_m. At $\tau = \tau_N = T$ there are pM intervals with computed data at $pM + 1$ spatial nodes. The role of p is to keep the lower accuracy tail of data at the nodes x_j, for j large, away from the domain of interest $(L, 0)$.

From these considerations it is clear that the number of operations involved at the m-th time step is of the order $pM + 2N - 2m$ and so the total cost of the algorithm is of the order,

$$
\text{cost} = \sum_{i=1}^{N} \left(pM + 2N - 2i \right) \;=\; O(pMN + N^2),
$$
$$
\leqslant \; C\big(pN^{4/3} + N^2\big).
$$

since, for stability, we need $\Delta t \leqslant C \Delta x^3$ (or $T/N \leqslant -CL^3/M^3$ giving $M^3 \leqslant -CL^3 N/T$) which means that $M = O(N^{1/3})$. We see that the cost is quadratic in N and so very high resolution solutions are beyond reach without either specialised computer power or by suffering long execution times. For example, a doubling of the spatial resolution from M to $2M$ will require increasing N to $8N$ to maintain stability. The cost therefore increases by a factor of 64.

To mitigate this both cores of a dual-core GNU/Linux (openSuSE 10.3) PC were exploited in a parallel solve (we used *OpenMP*, see `www.openmp.org`, with the GNU compiler `g++`).

In each of Figures 5, 7 and 6 we solved in $(L, 0) = (-700, 0)$ with $M = 14000$ and over $(0, T) = (0, 70)$ with $N = 700000$. We took $\widehat{M} = 10M + 2N = 1540000$ resulting in $\widehat{L} = -77000$.

References

[1] M. Abramowitz and I. Stegun. Handbook of Mathematical Functions. Dover, New York (1965)

[2] M.M. Cavalcanti, V.N. Domingos Cavalcanti and F. Natali. Exponential decay rates for the damped Korteweg-de Vries type equation. (To appear)

[3] A. Faminskii. Quasilinear evolution equations of the third order. *Bol. Soc. Parana. Mat.* (3) 91-108 (2007)

[4] B. Fornberg and G.B. Whitham. A numerical and theoretical study of certain nonlinear wave phenomena. *Phil. Trans. Roy. Soc. Lon.* Vol. 289, 373-404 (1978)

[5] A.V. Gurevich and L.P. Pitaevskii. Decay of initial discontinuity in the Korteweg-De Vries equation. *ZhETF Pis. Red.* Vol. 17, No. 5, 268-271 (1973)

[6] S. Kichenassamy and P.J. Olver. Existence and nonexistence of solitary wave solutions to high-order model evolution equations. *SIAM J. Appl. Math.* 23, 1141-1166 (1992)

[7] J.A. Leach. The large-time development of the solution to an initial-boundary value problem for the Korteweg-de Vries equation. I. Steady state solutions. *J. Differential Equations* 246 (9) 3681-3703 (2009).

[8] J.A. Leach. The large-time development of the solution to an initial-boundary value problem for the Korteweg-de Vries equation on the negative quarter-plane. *J. Differential Equations* 247 (4) 1206-1228 (2009).

[9] J.A. Leach and D.J. Needham. The large-time development of the solution to an initial-value problem for the Korteweg-de Vries equation: I. Initial data has a discontinuous expansive step. *Nonlinearity* 21, 2391-2408 (2008)

[10] J.A. Leach and D.J. Needham. Matched Asymptotic Expansions in Reaction-Diffusion Theory. Springer Monographs in Mathematics (2003)

[11] F. Linares and A.F. Pazoto. Asymptotic behaviour of the Korteweg-de Vries equation posed in a quarter plane. *J. Differential Equations* 246 (4) 1342-1353 (2009)

[12] H. Liu and M. Slemrod. KdV dynamics in the plasma-sheath transition. *Appl. Math. Lett.* 17 (4), 401-410 (2004)

[13] H. Liu and J. Yan. A local discontinuous Galerkin method for the Korteweg-de Vries equation with boundary effect. *Journal of Computational Physics* 215, 197-218 (2006)

[14] T.R. Marchant and N.F. Smyth. The initial boundary problem for the Korteweg-de Vries equation on the negative quarter-plane. *Proc. R. Soc. Lond.* A 458, 857-871 (2002)

[15] G.B. Whitham. Non-linear dispersive waves. *Proc. Roy. Soc.* A283, 238-291 (1965)